Chapter 1
On the Assumption of Laminar flow in Physiological Flows: Cerebral Aneurysms as an Illustrative Example

Øyvind Evju and Kent-Andre Mardal

1.1 Introduction

Most fluid flows in our human body, except for the blood flow in heart and aorta, are believed to be laminar in healthy individuals. A good reason for this, from an evolutionary point of view, is that turbulence introduces extra friction and hence transport is more efficient in the laminar regime than in the turbulent regime. It has also been shown that laminar flow ensures a healthy mechanotransduction[1] in the vessel walls. On the other hand, various pathologies, like for example atherosclerosis and aneurysms, involve anatomies causing disturbed flow and possibly even turbulent flow. The disturbances trigger a downward spiral where the disturbed flow leads to an unhealthy mechanotransduction causing remodelling of the vasculature which again worsen the flow disturbances. Recent research has therefore challenged the assumption of laminar flow in such pathologies and put the focus on the possible role of transitional or turbulent flow in these pathologies.

Transition to turbulence in steady pipe flow occurs at Reynolds number (Re) around 2300, while fully developed turbulence is obtained around 4000. The Reynolds number in large arteries and also elsewhere in our body is usually far below 2300 and laminar flow is therefore usually assumed. However, both the pulsatile nature of the flow and deviations from straight pipe geom-

Øyvind Evju
Simula Research Laboratory, P.O.Box 134, 1325 Lysaker, Norway,
e-mail: oyvinev@simula.no

Kent-Andre Mardal
Simula Research Laboratory, P.O.Box 134, 1325 Lysaker, Norway and
Department of Informatics, University of Oslo, P.O.Box 1080 Blindern 0316 Oslo,
e-mail: kent-and@simula.no

[1] Mechanotransduction refers to the process where cells convert mechanical stimuli to chemical activity and is vital in the remodelling that occur in vessels.

etry might introduce transition to turbulence at lower Reynolds numbers, as we will demonstrate in this chapter.

While the laminar regime and in many applications the fully developed turbulent regime are reasonably well understood from both a modelling and numerical point of view, the transitional regime with occasional turbulence poses additional challenges. Modelling is difficult in particular, because it is challenging to precisely predict the onset of the turbulent spots. Instead of modelling the turbulence, one might increase the resolution in space and time and resolve all scales of the turbulent flow numerically, a technique called direct numerical simulation (DNS). This approach is feasible only for flows with moderate Reynolds numbers because resolving the small structures (Kolmogorov microscales) induces computational costs scaling as Re^3. In addition to the high resolution requirement, it is necessary to employ schemes that introduce as little dissipation as possible. It may also be necessary to carefully construct the boundary conditions such that these allow for or induce small perturbations or unstable modes that may grow into turbulence. In numerical simulations that do not sufficiently address these requirements, transition is often not seen even though physical experiments reveal them under similar flow conditions.

This chapter is devoted to a critical review on the assumption of laminar flow in physiological flow applications and we will use blood flow in cerebral aneurysms as an illustrating example. We will discuss the consequences of this assumption, which lowers the requirement on the resolution and validates the use of stabilization techniques and time discretizations with dissipation. We will also review clinical and biomechanical findings suggesting that transitional flow is common or at least not unusual in many pathologies. Finally, we discuss cerebral aneurysms in depth and show that for some aneurysms transition may occur already for Reynolds number as low as 300.

1.2 On the definition of Turbulence

Defining and identifying transitional or turbulent flow in a pulsatile and complex 3D geometry is a challenging task. For completeness we include a formal definition of turbulence:

Turbulent flow is an irregular condition of flow in which the various quantities show a random variation with time and space coordinates, so that statistically distinct average values can be discerned.

The above definition was provided in [18] and later Bradshaw adds an important observation; namely that *turbulence has a wide range of scales.* See for example [46] for discussions concerning this definition. Following this definition we consider random fluctuations on a wide range of scales as the

defining characteristics of turbulence. Laminar flow on the other hand is characterized as smooth and deterministic.

Between the regimes of laminar and fully developed turbulent flows there is a regime with complex flow such as occasional turbulence or spots of turbulence that is often called the transitional regime. According to White [45, page 344] most analyses are devoted to either the fully developed turbulent regime or the laminar regime and engineers are advised to avoid the transitional regime. While engineers may choose to avoid this regime, several diseased states may lead to transitional flow and the unpredictability of transition may even be a factor that worsen the condition, as will be discussed in the following.

The distinction between laminar, transitional and turbulent flow dates back to 1883 when Osbourne Reynolds observed that the flow condition was governed by the ratio of inertial forces to viscous forces (the Reynolds number) in stationary pipe flow. In his famous experiments Reynolds showed that transition to turbulence in stationary pipe flow occurs at Re=2300 and fully developed turbulence is achieved at Re=4000. Subsequent experiments have shown that turbulence might be suppressed until Re=40 000 given sufficiently smooth pipe, inflow and outflow. On the other hand, the lower limit seems to be about 2000 [31].

Transitional or turbulent flow causes extra friction. For example, in stationary pipe flow the pressure drop needed to drive the flow under laminar conditions scales as V, where V is the mean flow, while in transitional or turbulent flow the pressure drop scales as $\approx V^{1.75}$. This was observed by Hagen in 1839 and is illustrated in Figure 1.1, see also [45, page 345]. As can be seen in this figure, the transition point is clearly defined as a sharp kink around $V = 1.1\,\mathrm{ft/s}$ which then gradually change to the fully developed turbulence at $V = 2.2\,\mathrm{ft/s}$. The transition point $V = 1.1\,\mathrm{ft/s}$ corresponds to Reynolds number 2100. The sharpness of the transition point suggests that the pressure drop might give insight into the precise transition point and we will therefore also discuss pressure drops in the following.

Pulsatility may both increase and decrease the threshold for transition. In particular, flow deceleration typically promote transition, while acceleration delay transition. Concerning flow in straight pipes, it was demonstrated in [40] that transition to turbulence is highly dependent on the Womersley number. Of particular importance for physiological flow is the fact that the transitional regime occur early for Womersley numbers between 2-5, numbers that are physiologically reasonable. Alternative definitions of the Reynolds number that put the focus on the pulsatility was proposed in this publication.

Probably even more important than the pulsatility is the geometry. For instance, in Couette flow or flow around cylinders, transition occurs at Re=500 and Re=300, respectively. For this reason a wide range of other Reynolds numbers has also been proposed in the literature, see [31] for an overview, but it remains difficult to employ these numbers as guidelines for when transition occurs in the complex vasculature of the body. Still, many works consider the

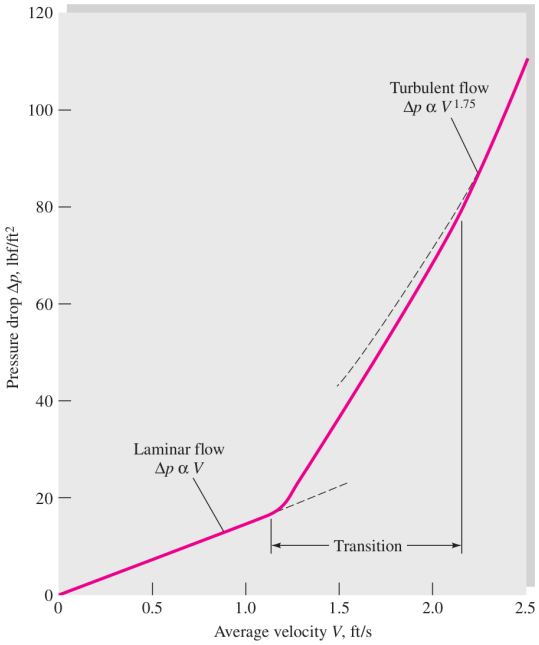

Fig. 1.1 The Figure is an illustration of Hagen's measurement of pressure drop in Poiseuille flow as a function of the fluid velocity.

Reynolds number as an important guideline for whether the flow is laminar or not and justify their laminar assumption by a Reynolds number calculation.

1.3 Clinical Observations

Clinically, turbulent blood flow has been observed in vivo associated with the heart valves, the ascending aorta, and in arteriovenous grafts. Audible sounds (20-20 000 Hz) caused by the high frequency pressure fluctuation of turbulence are for some conditions symptoms of severely disturbed flow. For instance heart murmurs are associated with turbulence generated by malfunctioning mitral valves or a stenosed aorta. Arteriovenous grafts sometimes produce audible thrills at frequencies 100-200 Hz caused by vein wall vibration.

Turbulence or transition have received less attention in other pathologies like atherosclerosis and aneurysms, but there are still significant evidence in the clinical literature suggesting that it is common or at least not unusual. For example, severe stenosis in the carotid artery can result in transition to turbulent flow, which may produce an audible sound (bruit) that physicians

can detect. Another manifestation of turbulence is pulsatile tinnitus, or tinnitus that is synchronous with a person's heartbeat, which are audible sounds that is transmitted to the inner ear [16]. This condition is likely caused by the abnormal blood flow associated with conditions such as arteriovenous malformations, stenosed carotid arteries, cerebral aneurysms etc. The topic of pulsatile tinnitus in association with cerebral aneurysms dates back to 1936 where Bergstrand et.al. [6] demonstrated pulsatile tinnitus in 4 of 22 cases of intra cranial aneurysms. While their relative high fraction of pulsatile tinnitus per aneurysms have been challenged in, e.g. Beadles [5], several resent studies report that pulsatile tinnitus is indeed present and caused by aneurysms [3, 35]. Pulsatile tinnitus, both subjective (as experienced by the patients) and objective (detected by the clinician), does however require that the sounds generated by the turbulent or transitional flow are transmitted either to the patients inner ear or through the the skull for detection. To improve the sound detection procedure, Ferguson employed a phonocatheter on the exposed aneurysm during craniotomy and found that 10 out of 17 aneurysms had bruits of sounds with predominate frequencies in the range of 270 to 660 Hz [10]. This suggests that a significant fraction of aneurysms may have transitional blood flow.

Clinicians have performed various glass model studies to consider the issue of turbulence in blood flow. Already in 1958, Stehbens [36] investigated the transition threshold in idealized bifurcations and S-shaped arteries modelling the carotid siphon. The critical Reynolds numbers in the bifurcation and the S-shaped geometry were 600 and 900, respectively. In all cases he used stationary inflow conditions. Later, in 1972, Roach et.al. [29] considered bifurcations and bifurcations with aneurysms at the apex using glass models and found that turbulence was present in bifurcations (depending on the angle of the bifurcation) at Re=1200 under steady conditions and around 800 under pulsatile condition. In aneurysms transition occurred already at Reynolds numbers between 400 and 500, with only a slight difference between stationary and pulsatile flow.

1.4 Mechanotransduction and the remodelling of the vasculature

The vasculature is an active system that adapt to facilitate a healthy blood flow. In particular, it seems that the arterial system adapt vessel radius to a flow that on average has a uniform wall shear stress (WSS) of around 5 Pa [13]. This finding is called the uniform WSS hypothesis and has been found to apply to most parts of the cardiovascular systems. Furthermore, bifurcations in most part of the vasculature have angles and radii that satisfy an optimum principle known as Murray's law. This law states that the energy requirements for metabolism and transport are minimized in blood flow.

Murray used this optimum principle to derive a relationship between angles and radii in bifurcations and this relationship has been validated in various parts of the cardiovascular in e.g. rats, dogs and humans [32, 48]. This law suggest that the cardiovascular system is tuned to be cost efficient. However, a notable exception from this law is the bifurcations associated with the circle of Willis, where cerebral aneurysms form [1, 20]. Hence, large parts of the vasculature appear to be constructed for an energy efficient transport of blood throughout the body. Moreover, the vasculature plays an active role and remodel itself to optimize the flow and maintain a uniform WSS. An example of this process can be found in [19, 26]. Here, the authors surgically closed both of the carotid arteries in a rabbit. The consequence was an increased flow of about 400% in the basilar artery. Over the course of a week, the artery grew radially until a baseline WSS was again obtained and the artery remained rather unchanged in the following weeks. The basilar artery is shown in Figure 1.2. Complex geometries like many bifurcations lead to deviations from the principle of uniform WSS and are particularly prone to e.g. atherosclerosis [23] and aneurysms [1]. These complex geometry also often cause early transition.

Fig. 1.2 The growth of the basilar artery in a rabbit before (left) and after (right) the closing of both of the carotid arteries. The figure is taken from [26].

Research on the mechanotransduction, the process where living cells turn mechanical stimuli to chemical signals, have firmly established that endothelial cells (EC), the cells that surface the innermost layer of the blood vessels, play an active role in the remodelling of blood vessels. Experiments have shown that EC respond to flow, and in particular that undisturbed flow leads to healthy remodelling, while disturbed or oscillating flow fail to do so [4, 7]. Turbulent shear stress also substantially increases the endothelial cell turnover when compared to laminar flow with similar shear [8].

It is however an open question at what time scales the mechanotransduction occur. The biomechanical signalling of EC involves reaction-diffusion process that are slow (tens of seconds) compared to the high-frequency fluctuations in blood flow. However, recent research suggest that the mechanical

signaling can be transmitted more rapidly (within 100 ms) through the cytoskeletal filaments within the EC layer and allow for rapid transmission over longer distances. Furthermore, there is evidence that also the medial and adventitial layers are responsive to this mechanical signalling [4]. It is, however, not known precisely how the various vessel layers remodel themselves and to what extent there are individual variations in the mechanotransduction and remodelling.

Finally, turbulent blood flow introduce clot formation. In fact, in [37] they generated turbulent flow in canine models and it was found that the weight of the thrombosis was proportional to the Reynolds number and turbulence intensity.

1.5 Modelling of blood flow

Blood is a suspension of blood cells, platelets and plasma and does therefore not necessarily display a Newtonian rheology. A wide range of different models have been proposed and analysed, see e.g. [30]. For blood flow in larger arteries and aneurysms, Newtonian models typically capture the main flow quite accurately, for example maximal WSS, average WSS and area of low WSS correlate strongly (>0.95) between Newtonian and commonly used non-Newtonian models [9], but may overestimate WSS in areas of low shear [47].

In large arteries there is also a pulsatile response in the vessel to the blood flow, and this fluid-structure interaction has been the subject of many recent publications [27, 28]. The pressure propagation throughout the vasculature can only be described by fluid-structure interaction models, but there is evidence that the main flow in localized regions can often be modelled by assuming rigid vessels. The main reason for this is that for localized vessel segments the whole segment deforms in synchrony [38]. Hence, for modelling of main flow features in large localized arteries it appears that Newtonian modelling with rigid vessels may be adequate under the assumption of laminar flow, bearing in mind the large flow differences caused by the geometrical variations between different patients.

The previously mentioned studies that report turbulence, all consider Newtonian flow within rigid geometries. However, both non-Newtonian viscosity and fluidstructure interaction may both delay or accelerate transition. From an engineering point of view, delay of transition has been a hot topic for over 50 years because of its potential to reduce drag and suppress noise.

Concerning transition and fluid–structure interaction, Kramer [22] demonstrated already in 1960 that compliant coating, based on the dolphin's epidermis, may substantially delay transition. Naturally, this spurred a lot of research activity, which mostly failed to reproduce the drag reduction demonstrated by Kramer. Now, more than 50 years after the initial experiments of Kramer, there is little doubt that compliant coating may delay transition,

c.f. e.g., [14]. Reynolds numbers for transition in geometries with compliant coating may exceed corresponding Reynolds numbers for flow within rigid geometries by more than an order of magnitude. However, it is also clear that delaying transition is delicate and that compliance might even introduce instabilities.

An interesting case here is the audible sounds caused by vein wall vibration in arteriovenous grafts. The vein wall vibration is present in vivo and is believed to be caused by high frequency pressure fluctuation in the turbulent blood flow occurring already at Reynolds number as low as 500. However, in vitro models and also numerical simulations have failed to demonstrate turbulent flow in models of arteriovenous grafts at such low Reynolds numbers [34]. In fact, the studies suggest that the graft geometry and flow pulsatility are not sufficient to explain the transition at such low Reynolds numbers and it appears that the only likely explanation is either the non-linear viscosity of blood or the compliance of the vessel walls. In particular, the high frequency content of the vortical structures appear to be strongly linked with the natural harmonics of the wall. We also remark that in arteriovenous grafts there is a strong correlation between vein wall vibration and intimal thickening [11], suggesting that the veins are able to sense and react to the turbulence although not in a beneficial manner.

1.6 On the modelling of transitional flow

The process of transition is a difficult topic that has been under intensive research since Reynolds and Hagen did their famous experiments. Transition occurs because unstable modes are triggered, starting often as minor perturbations to the flow that grow either in space, time or both. The Navier-Stokes equations are non-linear and non-normal and a consequence is that the standard approach of stability analysis in terms of eigenvalue fail to predict the occurrence of unstable mode leading to transition. For instance, transition in simple flow problems as Couette and Poiseuille can not be explained in terms the linear analysis of eigenvalues [41]. Because the exact mechanism behind transition (or the procedure to calculate the unstable modes) is not known, it is difficult to model transition using for instance Reynolds averaged Navier-Stokes equations for transition even though they often are powerful tools for fully developed turbulence.

For flow problems such as physiological flow applications where the Reynolds number is moderate, it is usually not possible to predict whether transition will occur or not. The only feasible approach seems to be to perform a DNS. This is, however, challenging for at least three reasons: 1) special care needs to be taken to construct discretization schemes to avoid dissipation, 2) the resolution needs to be extremely high compared to corresponding laminar

simulations, and 3) boundary conditions needs to be chosen such that instabilities are allowed.

This is in sharp contrast to simulations where laminar flow is assumed and where most simulations, at least for aneurysms studies, employ first order schemes with built-in dissipation that avoid stability issues [42]. Here, the justification for these schemes is that laminar flow is assumed. Moreover, as Valen-Sendstad and Steinman [42] point out, convergence studies are not always reported or are performed in a poor fashion. It is therefore difficult to determine whether transition would occur at a higher resolution in these studies. A recent benchmark study [39], where 25 research groups performed CFD analysis in a prescribed geometry of a cerebral aneurysm with a proximal stenosis given boundary conditions, reveals that the flow varied remarkably inside the aneurysms among the results of the different research groups. There was a clear tendency that simulations with research codes on high resolutions demonstrated flow instabilities to a greater extent than low resolution simulations performed with commercial codes.

Concerning the resolution of the discretization, the requirement of a DNS is that the so-called Kolmogorov scales are resolved. Determining the Kolmogorov scale is challenging from a numerical point of view as it needs to be estimated based on the simulation results, and grid independence of local quantities needs to be established. However, as pointed out in [2], performing DNS studies that concern blood flow is particularly challenging as the Kolmogorov length scale may be on the same scale as the red blood cells and thus it is on the scale where the continuum hypothesis breaks down.

Still, several attempts of DNS studies in carotid arteries [24], arteriovenous grafts [25], cerebral aneurysms [43] have been performed, albeit at a much coarser resolution than the estimates provided in [2]. These simulations report cycle-to-cycle variations on a wide range of scales, e.g., temporal fluctuations in the range of 100-1000 Hz. An important observation is that instabilities seems to be caused by geometry rather than the pulsatility and therefore that stationary inflow/outflow conditions can be used to detect possible transition effects and for grid-independence studies, c.f. e.g. [24, 42, 44]. This is because the pulsatility is relatively slow as compared with the velocities in the sense that the number of flow-throughs per cycle is sufficiently high. However, it has been pointed out that transition most often occurs in the deceleration phase [43]. Simulations with constant flow can therefore be assumed to predict a higher critical Reynolds number, than a similar simulation with pulsatile flow.

1.7 An illustrating example: Transition in a Cerebral Aneurysm

To investigate the threshold to transition, we consider an aneurysms from a canine model [21]. The aneurysm, although artificially produced, is a prototype for human aneurysms created by a technique often used in clinical trials. The aneurysm is shown in Figure 1.3.

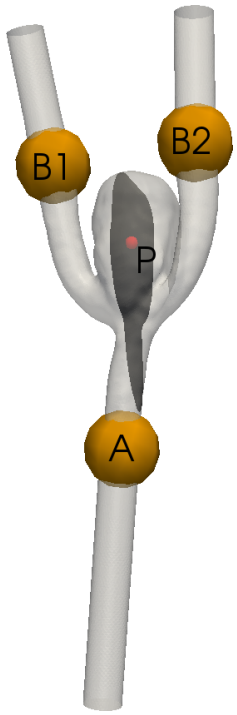

Fig. 1.3 The canine aneurysm that is used in our computations. The dark slice is used to display the flow field, the red dot denoted by a P shows the point used in our analysis of the turbulent characteristics, and the balls A, B1 and B2 are used to calculate the pressure drop over the aneurysm $\left(\Delta p := \bar{p}_A - \frac{\bar{p}_{B1}+\bar{p}_{B2}}{2}\right)$.

The aneurysm model was meshed with 3,275,000 tetrahedra, with a coarser mesh at the distal parts of the geometry. This corresponds to approximately 25-50 cells across the parent artery diameter and 120-150 cells across the diameter of the aneurysm, with an average edge length of 0.137mm. This is not claimed to be fully converged, as Figure 1.4 illustrates, but it is in the upper range of resolutions used in CFD studies within the field. However, to capture any high-frequency flow effects, the time step was set to 7.5e-6s,

several orders of magnitude below what is typically employed. Blood was modelled with a density of 1056 kg/m^3 and a Newtonian viscosity of 3.45 mPa s.

Dirichlet boundary conditions were set for the velocity, with no-slip conditions at the walls, and paraboloid-shaped inflows and outflows, with the flow rate distributed evenly between the two outflows. For the pressure, natural boundary conditions were used, and the resulting pressure was normalized around zero.

As was demonstrated in [12, 24], the transition to turbulence in larger arteries is predominantly governed by the geometry rather than the relatively slow pul- satility that merely turns the turbulence on and off. That is, given the relatively long cardiac cycle ($>$ 10 flow-throughs in a typical model), it is preferable to consider the question of turbulence under static conditions, which is done in the following. Notice, however, that while the boundary conditions are static, as the Reynolds number increase, the flow inside the aneurysm and surrounding will not be stationary. In fact, as was demonstrate in [44], we might expect high frequency fluctuations (>100 Hz) already at Reynolds numbers around 200-300.

The Navier-Stokes equations were solved with a finite element incremental pressure correction scheme, following the idea of [15]. The scheme applies a Crank-Nicolson method for the time stepping and a linear handling of the convection term as introduced by [33], making the tentative velocity step second order in both time and space. This scheme is chosen because it preserves the exact same stability properties as Navier-Stokes and hence does not introduce additional dissipation in the flow. The scheme reads as:

At $t = t^{n+1} := (n+1)\Delta t$ with the solution $(u^k, p^k) := (u(t^k), p(t^k))$ known for $k = 0, ..., n$, kinematic viscosity ν, and density ρ, do

1. Solve a reaction-diffusion-advection equation for a tentative velocity, $\tilde{u}^{n+1}$:

$$\frac{1}{\Delta t}\left(\tilde{u}^{n+1} - u^n\right) - \nabla \cdot \nu \nabla \tilde{u}^{n+\alpha} + u^* \cdot \nabla \tilde{u}^{n+\alpha} + \nabla p^{n-1} = 0,$$

where

$$\tilde{u}^{n+\alpha} = \alpha \tilde{u}^{n+1} + (1-\alpha)\, u^n \ (\alpha = \tfrac{1}{2} \text{ for Crank-Nicolson}),$$
$$u^* = \frac{3}{2}u^n - \frac{1}{2}u^{n-1}.$$

2. Solve a Poisson equation for the pressure, p^{n+1}:

$$\Delta p^{n+1} = \Delta p^n + \frac{\rho}{\Delta t}\nabla \cdot \tilde{u}^{n+1}.$$

3. Update for the correct velocity, u^{n+1}:

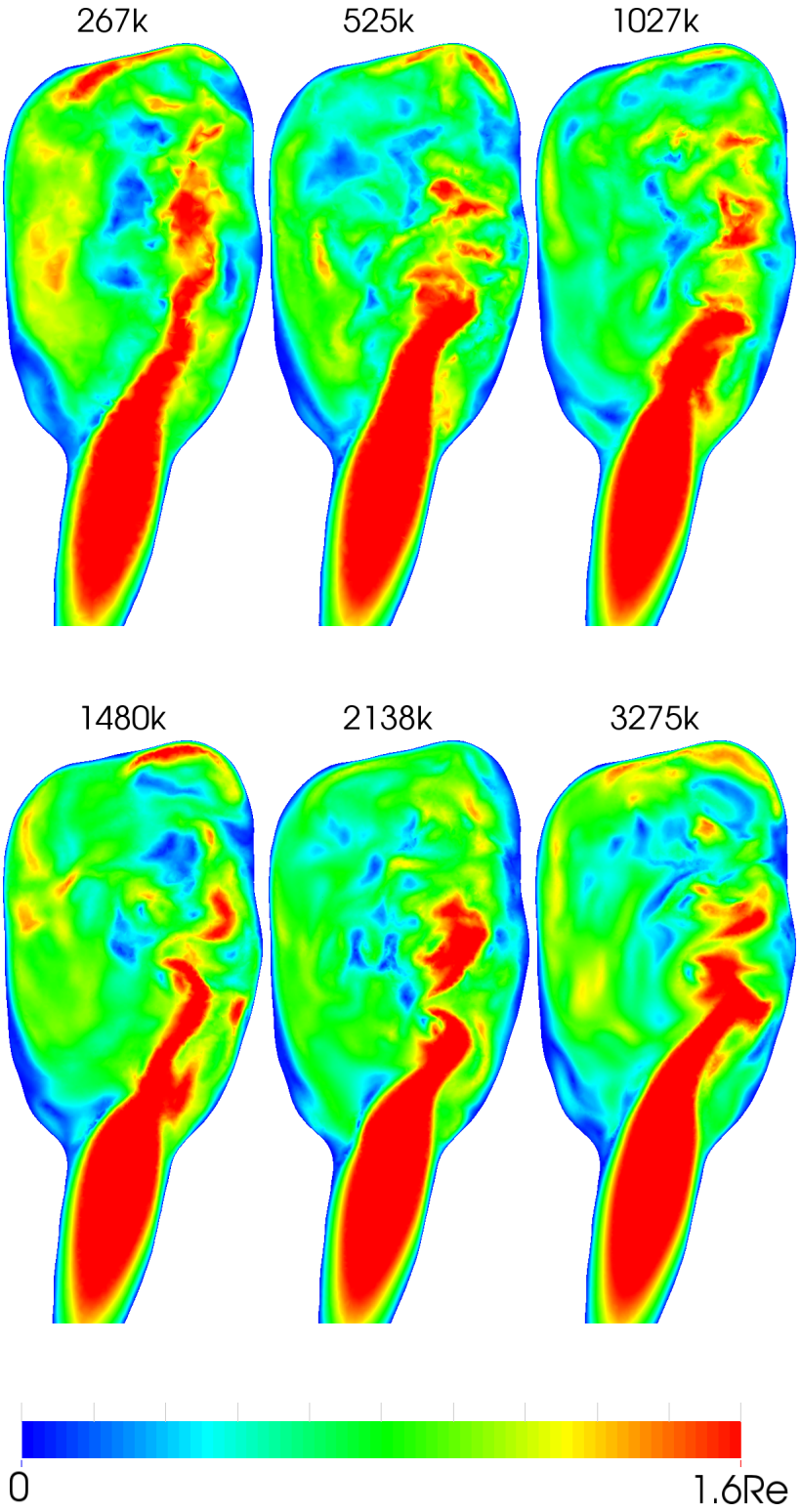

Fig. 1.4 The Figure shows the velocity magnitude in a slice through the aneurysm at Reynolds numbers 1000 at various resolutions.

$$u^{n+1} = \tilde{u}^{n+1} - \frac{\Delta t}{\rho} \nabla \left(p^{n+1} - p^n \right).$$

4. Increment $(n \leftarrow n+1)$ and repeat.

The scheme was implemented in the open source software package FEniCS[2], and is available through the open source CFD package *cbc.flow*[3]. Linear elements were used for both velocity and pressure.

We first ran simulations at a coarser time resolution to obtain steady state solutions to be used as initial condition for our main simulations with 0.2 to 6 flow-throughs depending on the Reynolds number. We then disregarded the first 5000 time steps of our main simulations to allow for the finer time scales to reach a quasi-steady state.

To analyse the turbulent characteristics of the flow over time, we analyse the power spectral density (PSD) of the velocity magnitude in a point of the interior of the aneurysm sac, as shown in Figure 1.3. The PSD for a discrete time-signal is as follows. Let

$$S_{xx}(\omega) = \frac{(\Delta t)^2}{T} \left| \sum_{n=1}^{N} x_n e^{-i\omega n} \right|^2,$$

where ω is the frequency, Δt is the time step, T is the time interval, N is the number of samples and x_n denotes the sample at $t = n\Delta t$. Since the velocity magnitude is real-valued, the PSD is symmetric, i.e. $S_{\|\mathbf{u}\|\|\mathbf{u}\|}(\omega) = S_{\|\mathbf{u}\|\|\mathbf{u}\|}(-\omega)$. We therefore define $PSD_{\|\mathbf{u}\|}$ as

$$PSD_{\|\mathbf{u}\|}(\omega) := 2S_{\|\mathbf{u}\|\|\mathbf{u}\|}(\omega), \qquad \omega > 0.$$

This is related to the sample variance of $\|\mathbf{u}\|$ with the relation

$$\sigma^2 = \int_0^\infty PSD_{\|\mathbf{u}\|}(\omega)\, d\omega.$$

Thus, $PSD_{\|\mathbf{u}\|}$ can provide information about which frequencies are required to resolve, in our case, the pointwise velocity magnitude. In the following, we report $\omega_{0.95}$ as the approximate frequency that is required to capture 95% of the variance, that is,

$$\int_0^{\omega_{0.95}} PSD_{\|\mathbf{u}\|}(\omega)\, d\omega = 0.95\sigma^2.$$

[2] http://fenicsproject.org

[3] https://bitbucket.org/simula_cbc/cbcflow

Given our time stepping, we are limited by the Nyquist frequency of $\frac{1}{2\Delta t} \approx 66667$ Hz. The number of bins in the discrete Fourier transform are given by $T\frac{1}{2\Delta t} = 20000$, and the bin size is thus 3.33 Hz.

The PSD analysis seen in Figure 1.5 revealed a significant change in the frequencies of the flow between Re=250 and Re=500. When Re<250, $\omega_{0.95}$ is less than 60 Hz, but this jumps to 313 Hz at Re=500 and further to 923 Hz and 2046 Hz at Re=1000 and Re=2000, respectively. To capture any flow effects at these frequencies, the resolution requirements are minimum twice the reported frequency. However, this is no guarantee for the *correct* flow effects at these frequencies. It should also be noted that when considering pulsatile flows, the frequencies present in the flow are likely significantly higher, due to the deceleration phase of the flow at late systole/early diastole.

Considering the slice views in Figure 1.6, the pattern is clearly seen of the increasing complexity in the flow from Re=250 and upwards. Worth noting is also the flow field in the parent artery, which appears laminar as expected.

While blood displays non-Newtonian rheology, in many CFD studies the shear rates are assumed adequately high to assume a Newtonian behaviour. While this assumption is often adequate [9], its effect on the transition of flow has not been studied. To address this, we employ a Modified Cross viscosity presented in Figure 1.7. The model parameters are fitted to viscometer data [30], and the computation was done explicitly. We re-ran simulations at the flow rates corresponding to Re=250 and Re=500 in the Newtonian case. Since the flow rates are equal, but the viscosity is not, the actual Reynolds number is somewhat lower for the non-Newtonian case. The Reynolds number will be similar to the Newtonian case in the parent artery, where the shear rate is high, but will change in the parts of the geometry where the shear rate drops. On average, the Modified Cross model predicted 20% higher viscosity compared to the Newtonian case.

The resulting PSD can be seen in Figure 1.8, with slice-views of the flow in Figure 1.9. Keeping in mind the effects on the Reynolds number, it would appear that the non-Newtonian viscosity model delays the transition of the flow significantly.

In pipe flow the transition to turbulence is clearly identified by a marked change in the pressure drop relation to velocity, as was shown in the previously mentioned Figure 1.1. Clearly the pressure drop increases linearly as the velocity (or Reynolds number) increase in laminar flow, but has a sharp point of transition that occur around Re=2000. Similarly, in Figure 1.10, we show the pressure drop as a function of the Reynolds number in the parent vessel. For Reynolds number between 0 and 200 the pressure drop demonstrate a linear dependency to the Reynolds number. However, already at Re=200 deviations start to occur, also with notable variations over time. The transition point is, however, not as easily identified as in stationary pipe flow.

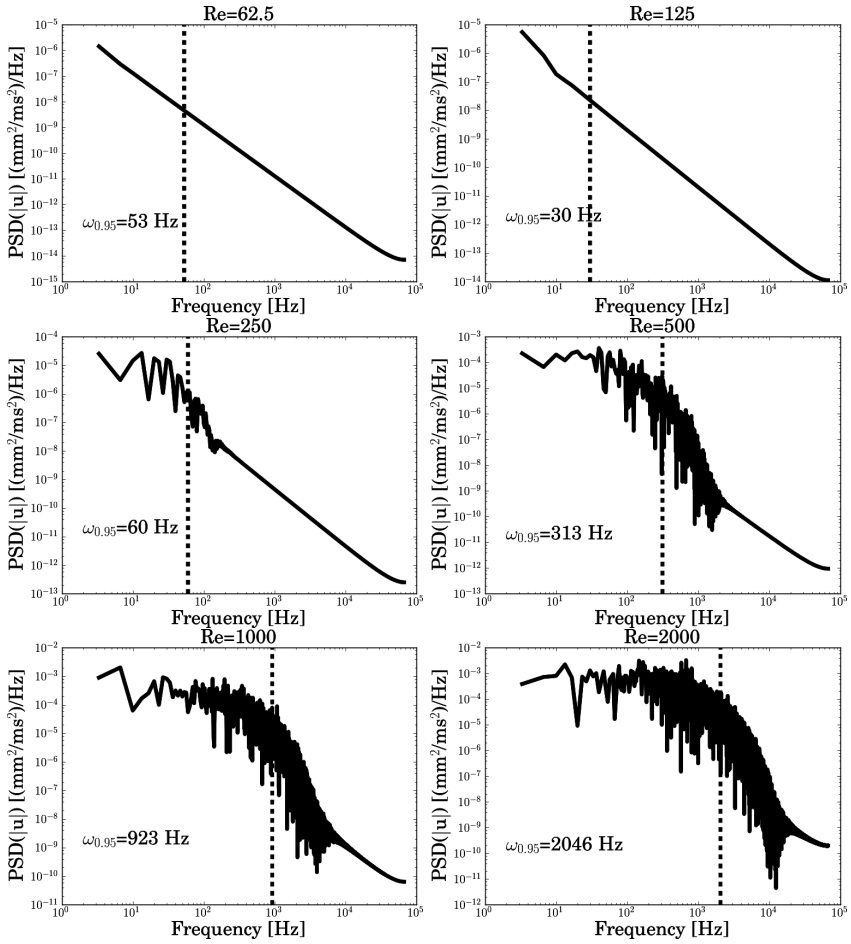

Fig. 1.5 The Figure shows the power spectrum of a point in the aneurysm at different Reynolds numbers.

1.8 Discussion

This chapter mainly discuss aspects of cerebral aneurysms and aim to illustrate that transition to turbulence might be an important factor for some aneurysms. We modelled a canine aneurysm model, under steady in- and outflow conditions, and transition occurred already at Reynolds number around 200-500. It remains to be investigated whether transition is important in vivo and whether it is linked to rupture.

Aneurysms have strong geometrical variation. A recent publication [44] found transition in 5 of 12 middle cerebral artery aneurysms at comparable Reynolds numbers (also under stationary conditions). Some clinical research

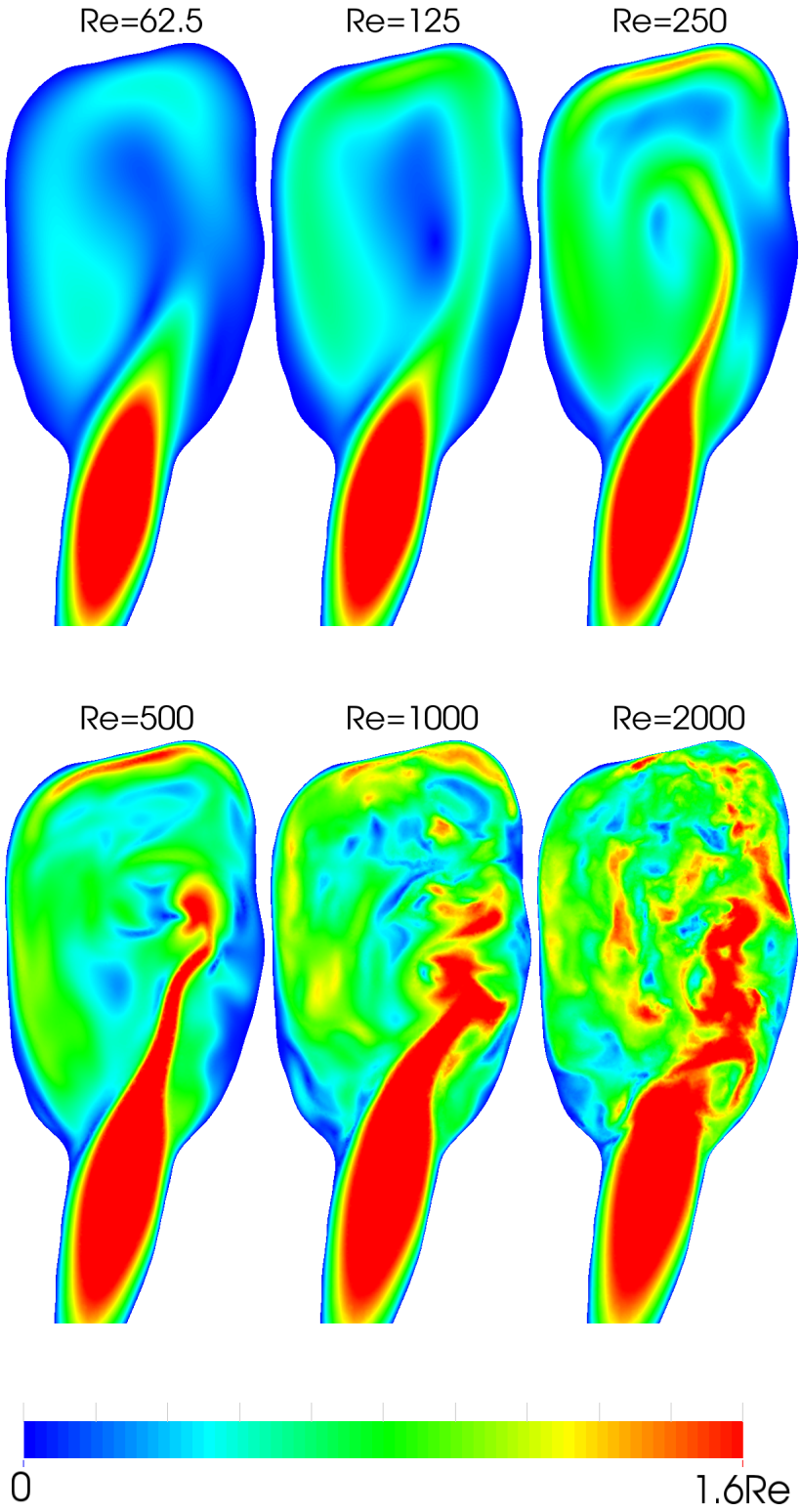

Fig. 1.6 The Figure shows the velocity magnitude in a slice through the aneurysm at different Reynolds numbers.

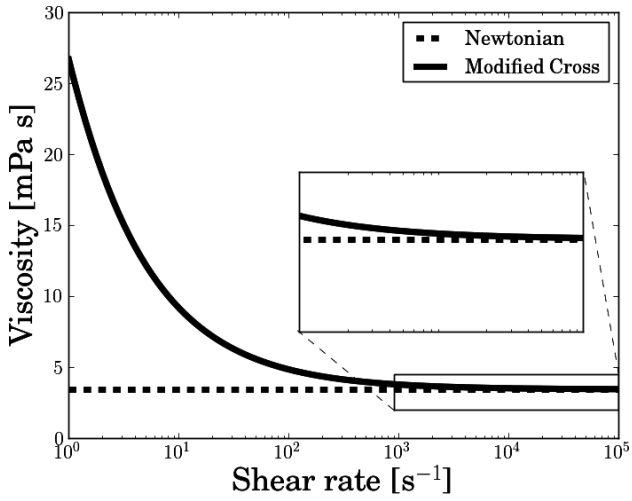

Fig. 1.7 The two viscosity models used. The Modified Cross model is given by $\frac{\mu-\mu_\infty}{\mu_0-\mu_\infty} = \frac{1}{(1+(l\dot{\gamma})^m)^a}$ with $l = 3.736s$, $m = 2.406$, $a = 0.254$, $\mu_0 = 0.056\,Pa\,s$, $\mu_\infty = 0.00345\,Pa\,s$. Note that the Modified Cross approaches the Newtonian model used as $\dot{\gamma} \to \infty$.

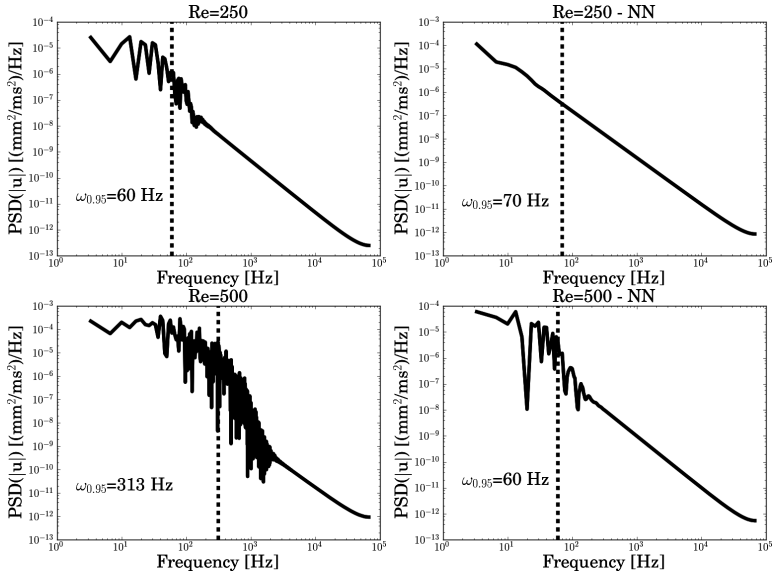

Fig. 1.8 The Figure shows the $PSD_{\|\mathbf{u}\|}$ Reynolds numbers 250 and 500 with a Newtonian and non-Newtonian viscosity model.

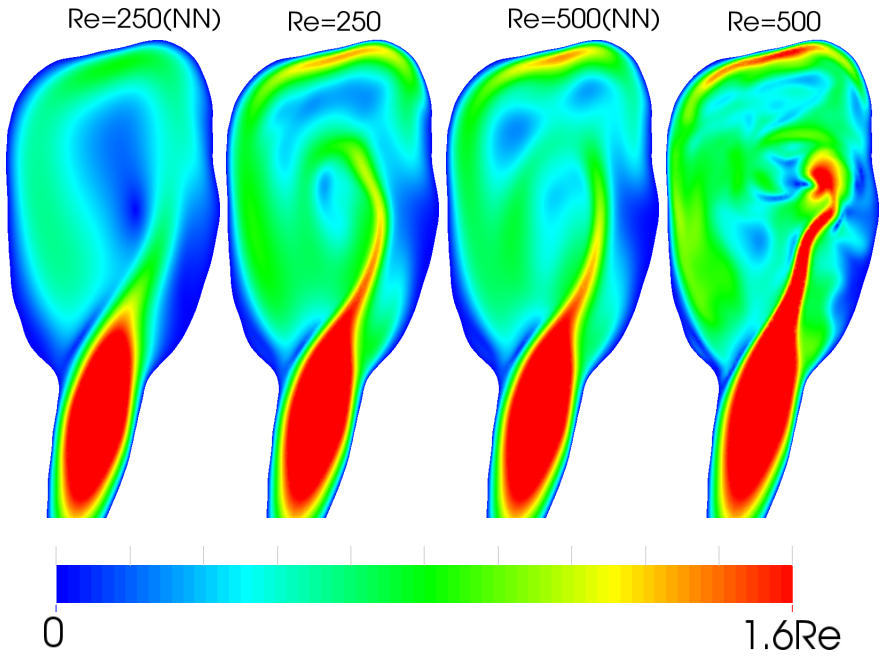

Fig. 1.9 The Figure shows the velocity magnitude of the flow for simulations with a non-Newtonian viscosity compared to simulations with a Newtonian viscosity.

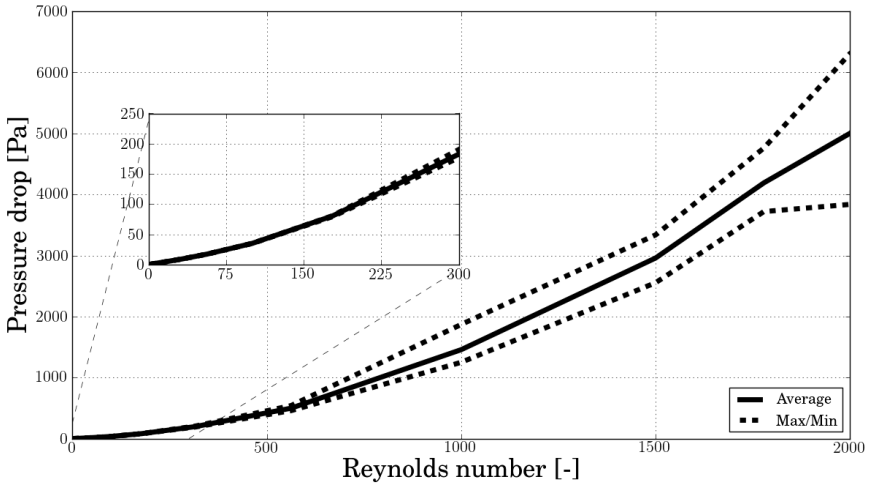

Fig. 1.10 The figure shows the pressure drop over the aneurysm as a function of the Reynolds number. Clearly, the pressure drop demonstrate a close to linear relation with respect to the Reynolds number for low numbers, but already at around Reynolds number 200 deviations from the linear relation occur and the pressure drop is no longer static in time.

have also reported signs of transition. For instance, Ferguson found that 10 out of 17 aneurysms had bruits of sounds with predominate frequencies in the range of 270 to 660 Hz [10] and suggested that the sounds were generated by transitional or turbulent flow inside the aneurysm. Other studies such as [3, 6, 35] suggest that pulsatile tinnitus sometimes is caused by transition to turbulent flow inside aneurysms.

There are many factors that may both promote and delay transition. In addition to the geometry, both flow pulsatility, non-Newtonian rheology, and fluid–structure interaction between blood and vessels may significantly both decrease and increase the threshold for transition. Furthermore, these factors may even promote transition in some aneurysm and delay transition in others. In this paper, we have demonstrated that a non-Newtonian model (Modified Cross) delayed transition in one particular aneurysm. It is not clear whether this applies to other aneurysm or non-Newtonian models.

Many other conditions related to abnormal blood flow, such as stenosed carotid arteries, aortic aneurysms, arteriovenous malformation share the characteristics of Reynolds number significantly less than 2000, but involve flow in highly complex geometry that might significantly reduce the threshold of transition. Furthermore, audible sounds are often indicative of the severity of the conditions. It therefore seems that transitional or turbulent flow may be associated with many cardiovascular conditions and this observation suggest that an increased focus on transition in the computational modelling community might be needed.

The flow of cerebrospinal fluid flow that surrounding the central nervous system is in many respect similar to cardiovascular flow. Rough calculations of the Reynolds number suggest that it is around 200 in healthy flow, but several conditions are associated with hyper-kinetic flow. Clinicians often report turbulence in normal pressure hydrocephalus, a form of dementia. A recent publication [17] shows that the cerebrospinal fluid flow is on the threshold to transition in a patient with the Chiari malformation - a condition where the lower part of the brain is herniated through the skull and obstruct the pulsatile flow between the neck and skull. Hence, transition may also be an issue for conditions associated with abnormal cerebrospinal fluid flow.

Detecting transitional or turbulent flow by performing numerical simulations are challenging because the mechanism behind transition is only partly understood. Delaying or removing transition in numerical simulations are easily done by for example employing stabilizing schemes or using too coarse resolution. However, clinical evidence over a wide range of applications suggest that flow instabilities, transition and turbulence might be important in several conditions. Finally, the fluid-structure interaction between the flow and surrounding tissue and the non-linear viscosity of blood might both stabilize and de-stabilize the flow depending on the circumstances. Hence, at this point, it seem that there are many open questions and unresolved issues concerning transitional flow in several important diseases.

1.9 Conclusion

Some evidence in the clinical literature suggest that conditions such as for example cerebral aneurysms may sometimes cause transition to turbulence. Still, this issue has largely been neglected in the biomechanical modelling and numerical simulations. The current chapter present simulations that demonstrate that transition may occur already at Reynolds number of the order of 300-500 in a typical canine model aneurysm. Aneurysm geometry, flow pulsatility, non-Newtonian rheology, and fluid–structure interaction may both promote and delay transition and it is therefore unclear how important transition is in vivo.

References

[1] M. S. Alnæs, J. Isaksen, K.-A. Mardal, B. Romner, M. K. Morgan, and T. Ingebrigtsen. Computation of hemodynamics in the circle of willis. *Stroke*, 38(9):2500–2505, 2007.

[2] L. Antiga and D. A. Steinman. Rethinking turbulence in blood. *Biorheology*, 46(2):77–81, 2009.

[3] J. Austin and D. Maceri. Anterior communicating artery aneurysm presenting as pulsatile tinnitus. *ORL; Journal for oto-rhino-laryngology and its related specialties*, 55(1):54–57, 1993.

[4] A. I. Barakat. Blood flow and arterial endothelial dysfunction: Mechanisms and implications. *Comptes Rendus Physique*, 2013.

[5] C. F. Beadles. Aneurisms of the larger cerebral arteries. *Brain*, 30(3): 285–336, 1907.

[6] H. Bergstrand, H. Olivecrona, and W. Tönnis. *Gefässmissbildungen und Gefässgeschwülste des Gehirns*. Georg Thieme, 1936.

[7] S. Chien. Mechanotransduction and endothelial cell homeostasis: the wisdom of the cell. *American Journal of Physiology-Heart and Circulatory Physiology*, 292(3):H1209–H1224, 2007.

[8] P. F. Davies, A. Remuzzi, E. J. Gordon, C. F. Dewey, and M. A. Gimbrone. Turbulent fluid shear stress induces vascular endothelial cell turnover in vitro. *Proceedings of the National Academy of Sciences*, 83(7):2114–2117, 1986.

[9] Ø. Evju, K. Valen-Sendstad, and K.-A. Mardal. A study of wall shear stress in 12 aneurysms with respect to different viscosity models and flow conditions. *Journal of biomechanics*, 46(16):2802–2808, 2013.

[10] G. G. Ferguson. Turbulence in human intracranial saccular aneurysms. *Journal of neurosurgery*, 33(5):485–497, 1970.

[11] M. F. Fillinger, E. R. Reinitz, R. A. Schwartz, D. E. Resetarits, A. M. Paskanik, D. Bruch, and C. E. Bredenberg. Graft geometry and ve-

nous intimal-medial hyperplasia in arteriovenous loop grafts. *Journal of Vascular Surgery*, 11(4):556–566, 1990.

[12] P. F. Fischer, F. Loth, S. E. Lee, S.-W. Lee, D. S. Smith, and H. S. Bassiouny. Simulation of high-Reynolds number vascular flows. *Computer methods in applied mechanics and engineering*, 196(31):3049–3060, 2007.

[13] Y.-c. Fung. *Biomechanics: circulation*. Springer, 1997.

[14] M. Gad-el Hak et al. Compliant coatings: a decade of progress. *Applied Mechanics Reviews*, 49:S147–S160, 1996.

[15] K. Goda. A multistep technique with implicit difference schemes for calculating two-or three-dimensional cavity flows. *Journal of Computational Physics*, 30(1):76–95, 1979.

[16] F. Hafeez, R. L. Levine, and D. A. Dulli. Pulsatile tinnitus in cerebrovascular arterial diseases. *Journal of Stroke and Cerebrovascular Diseases*, 8(4):217–223, 1999.

[17] A. Helgeland, K.-A. Mardal, V. Haughton, and B. A. Pettersson Reif. Numerical simulations of the pulsating flow of cerebrospinal fluid flow in the cervical spinal canal of a chiari patient. *Journal of Biomechanics*, 2014.

[18] J. Hinze. *Turbulence*. McGraw-Hill Book Company, 1959.

[19] Y. Hoi, L. Gao, M. Tremmel, R. A. Paluch, A. H. Siddiqui, H. Meng, and J. Mocco. In vivo assessment of rapid cerebrovascular morphological adaptation following acute blood flow increase. *Journal of neurosurgery*, 109(6):1141, 2008.

[20] T. Ingebrigtsen, M. K. Morgan, K. Faulder, L. Ingebrigtsen, T. Sparr, and H. Schirmer. Bifurcation geometry and the presence of cerebral artery aneurysms. *Journal of neurosurgery*, 101(1):108–113, 2004.

[21] J. Jiang, K. Johnson, K. Valen-Sendstad, K.-A. Mardal, O. Wieben, and C. Strother. Flow characteristics in a canine aneurysm model: A comparison of 4D accelerated phase-contrast MR measurements and computational fluid dynamics simulations. *Medical Physics*, 38:6300, 2011.

[22] M. O. Kramer. Boundary layer stabilization by distributed damping. *Journal of the American Society for Naval Engineers*, 72(1):25–34, 1960.

[23] D. N. Ku. Blood flow in arteries. *Annual Review of Fluid Mechanics*, 29(1):399–434, 1997.

[24] S. E. Lee, S.-W. Lee, P. F. Fischer, H. S. Bassiouny, and F. Loth. Direct numerical simulation of transitional flow in a stenosed carotid bifurcation. *Journal of biomechanics*, 41(11):2551–2561, 2008.

[25] S.-W. Lee, P. Fischer, F. Loth, T. Royston, J. Grogan, and H. Bassiouny. Flow-induced vein-wall vibration in an arteriovenous graft. *Journal of fluids and structures*, 20(6):837–852, 2005.

[26] H. Meng, D. D. Swartz, Z. Wang, Y. Hoi, J. Kolega, E. M. Metaxa, M. P. Szymanski, J. Yamamoto, E. Sauvageau, and E. I. Levy. A model system for mapping vascular responses to complex hemodynamics at arterial bifurcations in vivo. *Neurosurgery*, 59(5):1094, 2006.

[27] A. Quarteroni and L. Formaggia. Mathematical modelling and numerical simulation of the cardiovascular system. *Handbook of numerical analysis*, 12:3–127, 2004.

[28] A. Quarteroni, M. Tuveri, and A. Veneziani. Computational vascular fluid dynamics: problems, models and methods. *Computing and Visualization in Science*, 2(4):163–197, 2000.

[29] M. R. Roach, S. Scott, and G. G. Ferguson. The hemodynamic importance of the geometry of bifurcations in the circle of willis (glass model studies). *Stroke*, 3(3):255–267, 1972.

[30] A. M. Robertson, A. Sequeira, and R. G. Owense. Rheological models for blood. In *Cardiovascular mathematics. Modeling and simulation of the circulatory system*, pages 211–241. Springer-Verlag Italia, Milano, 2009.

[31] H. Schlichting and J. Kestin. *Boundary-layer theory*, volume 539. McGraw-Hill New York, 1968.

[32] T. F. Sherman. On connecting large vessels to small. The meaning of Murray's law. *The Journal of general physiology*, 78(4):431–453, 1981.

[33] J. Simo and F. Armero. Unconditional stability and long-term behavior of transient algorithms for the incompressible Navier-Stokes and Euler equations. *Computer Methods in Applied Mechanics and Engineering*, 111(1):111–154, 1994.

[34] D. S. Smith. *Experimental Investigation of Transition to Turbulence in Arteriovenous Grafts*. PhD thesis, University of Illinois at Chicago, 2008.

[35] G. Sonmez, C. C. Basekim, E. Ozturk, A. Gungor, and E. Kizilkaya. Imaging of pulsatile tinnitus: a review of 74 patients. *Clinical imaging*, 31(2):102–108, 2007.

[36] W. Stehbens. Turbulence of blood flow. *Experimental Physiology*, 44(1): 110–117, 1959.

[37] P. D. Stein and H. N. Sabbah. Measured turbulence and its effect on thrombus formation. *Circulation Research*, 35(4):608–614, 1974.

[38] D. A. Steinman. Assumptions in modelling of large artery hemodynamics. In *Modeling of Physiological Flows*, pages 1–18. Springer, 2012.

[39] D. A. Steinman, Y. Hoi, P. Fahy, L. Morris, M. Walsh, N. Aristokleous, A. S. Anayiotos, Y. Papaharilaou, A. Arzani, S. Shadden, et al. Variability of CFD solutions for pressure and flow in a giant aneurysm: The SBC2012 CFD challenge. *Journal of biomechanical engineering*, 1:542, 2013.

[40] J. Stettler and A. Hussain. On transition of the pulsatile pipe flow. *Journal of Fluid Mechanics*, 170(1):169–197, 1986.

[41] L. Trefethen, A. Trefethen, S. Reddy, T. Driscoll, et al. Hydrodynamic stability without eigenvalues. *Science*, 261(5121):578–584, 1993.

[42] K. Valen-Sendstad and D. Steinman. Mind the gap: Impact of computational fluid dynamics solution strategy on prediction of intracranial aneurysm hemodynamics and rupture status indicators. *American Journal of Neuroradiology*, 2013. doi: 10.3174/ajnr.A3793.

[43] K. Valen-Sendstad, K.-A. Mardal, M. Mortensen, B. A. P. Reif, and H. P. Langtangen. Direct numerical simulation of transitional flow in a patient-specific intracranial aneurysm. *Journal of biomechanics*, 44(16): 2826–2832, 2011.

[44] K. Valen-Sendstad, K.-A. Mardal, and D. A. Steinman. High-resolution cfd detects high-frequency velocity fluctuations in bifurcation, but not sidewall, aneurysms. *Journal of Biomechanics*, 46(2):402–407, 2013.

[45] F. M. White. *Fluid mechanics*. WCB/McGraw-Hill, Boston, 1999.

[46] D. C. Wilcox. *Turbulence modeling for CFD*, volume 2. DCW industries La Canada, 1998.

[47] J. Xiang, M. Tremmel, J. Kolega, E. I. Levy, S. K. Natarajan, and H. Meng. Newtonian viscosity model could overestimate wall shear stress in intracranial aneurysm domes and underestimate rupture risk. *Journal of NeuroInterventional Surgery*, 4(5):351–357, 2012.

[48] M. Zamir. Nonsymmetrical bifurcations in arterial branching. *The Journal of general physiology*, 72(6):837–845, 1978.